Journal of Electroanalytical Chemistry 785 (2017) 26–32

Contents lists available at ScienceDirect

Journal of Electroanalytical Chemistry

journal homepage: www.elsevier.com/locate/jelechem

Ultra-sensitive phenol sensor based on overcoming surface fouling of reduced graphene oxide-zinc oxide composite electrode

Rinky Sha [a], Sampath Kumar Puttapati [b], Vadali VSS Srikanth [b], Sushmee Badhulika [a,*]

[a] Department of Electrical Engineering, Indian Institute of Technology, Hyderabad 502285, India
[b] School of Engineering Sciences and Technology, University of Hyderabad, Gachibowli, Hyderabad 500046, India

ARTICLE INFO

Article history:
Received 27 September 2016
Received in revised form 30 November 2016
Accepted 1 December 2016
Available online 06 December 2016

Keywords:
Environmental sensors
Non-enzymatic
Phenol sensor
Reduced graphene oxide
ZnO

ABSTRACT

A major drawback of non-enzymatic approach for phenol detection is surface fouling which results from the electrochemical oxidation of phenol to polymeric products, thereby restraining the electrode process to low concentrations and limited to single time use. In this work, we report a novel approach for stable, non-enzymatic phenol detection using reduced Graphene Oxide (rGO)-Zinc Oxide (ZnO) composite modified Glassy Carbon Electrode (GCE) which eliminates the surface fouling effect by allowing precise selection of the sensing peak. Here, the rGO-ZnO composite was synthesized using a wet chemical method wherein rGO and ZnO were formed in-situ from GO and Zinc Acetate, respectively. The phenol sensing was investigated by differential pulse voltammetry (DPV) which yielded two peaks at 0.35 V and 0.94 V. Phenol detection was performed at a lower potential (0.35 V) as it eliminates the need for surface renewal of the electrode prior to each scan caused due to surface fouling thus facilitating stable and reproducible detection. The as-fabricated sensor responded linearly to phenol over two ranges, one in the range 2–15 μM with a ultrahigh sensitivity of 1.79 μA/μM cm^2 and the other in the range 15–40 μM with a sensitivity of 0.389 μA/μM cm^2 with good reproducibility, stability, selectivity and a lower detection limit of 1.94 μM. The sensing ability of rGO-ZnO modified GCE was studied in terms of forward biased nano Schottky barriers at the rGO-ZnO interface. This composite based sensor provides a low cost, non-enzymatic and voltammetric detection of phenol in industrial and environmental analyses.

1. Introduction

Phenol is a common organic contaminant found in air and water at very low concentrations. It is introduced into the environment through the effluents of chemical and industrial activities and its concentration in water bodies varies depending on its source (refineries: 0.06–5.3 mM, petrochemical industries: 0.03–13 mM, pulp and paper industries: 0.001–17 mM, etc.) [1–4]. It is considered as a priority pollutant in the field of environmental research due to its toxicity, bioaccumulation, environmental persistence, highly carcinogenic and mutagenic effects in aquatic organisms and humans causing damage to lungs, liver, kidney, central nervous system, human tissues and so on [5–6]. Due to these detrimental effects of phenol, the design and fabrication of sensors with enhanced sensitivity to detect and accurately quantify phenol at micro molar scale are of utmost importance.

Most common techniques employed for phenol detection include liquid and gas chromatography, capillary electrophoresis, flow injection analysis etc. [7–10] Despite their high sensitivity and selectivity, these techniques are expensive, require sophisticated instrumentation and time-consuming sample pretreatments, thereby being unsuitable for in situ and continuous measurements [2–4,11–12]. As a result, electrochemical sensors have attracted significant attention for direct detection of phenol due to their high sensitivity, faster response, low cost and ability to detect in situ in real time [6].

Electrochemical detection of phenol is performed on both enzymatic and non-enzymatic platforms. Disadvantages associated with enzymatic sensors include immobilization of enzymes, lack of reproducibility, and limited working conditions such as temperature, pH and humidity [2]. In non-enzymatic approach, phenol is detected through its oxidation on suitable electrodes at a positive potential. However, the phenoxy radicals (obtained due to phenol's oxidation) are further oxidized into polymeric contaminants which result in surface fouling of the electrode. As a result, preventing the electrode from deactivation remains a major challenge. To overcome this issue, novel electrode materials for non-enzymatic phenol detection have been reported [12–14]. In this work, we report such a new electrode material i.e., Reduced Graphene Oxide (rGO)-Zinc Oxide (ZnO) composite modified Glassy Carbon Electrode (GCE) for non-enzymatic sensing of phenol that simultaneously eliminates the operational challenges faced by conventional electrodes while offering enhanced sensitivity.

ZnO has been extensively used in electrochemical sensing due to its wide band gap (~3.2 eV) and high exciton binding energy (~60 meV),

* Corresponding author.
E-mail address: sbadh@iith.ac.in (S. Badhulika).

http://dx.doi.org/10.1016/j.jelechem.2016.12.001
1572-6657/

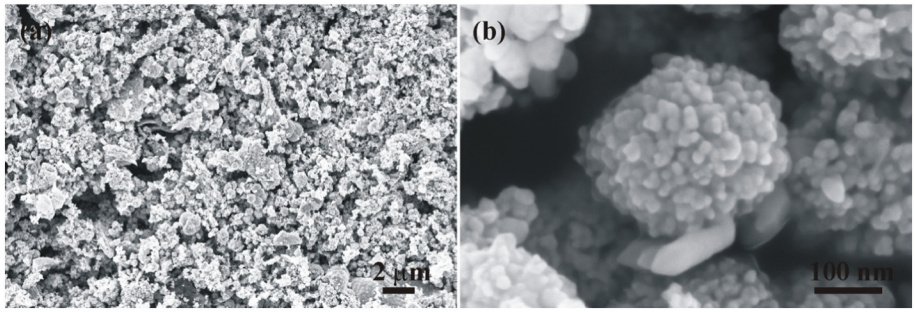

Fig. 1. (a) Low and (b) high magnification FESEM images of rGO-ZnO composite.

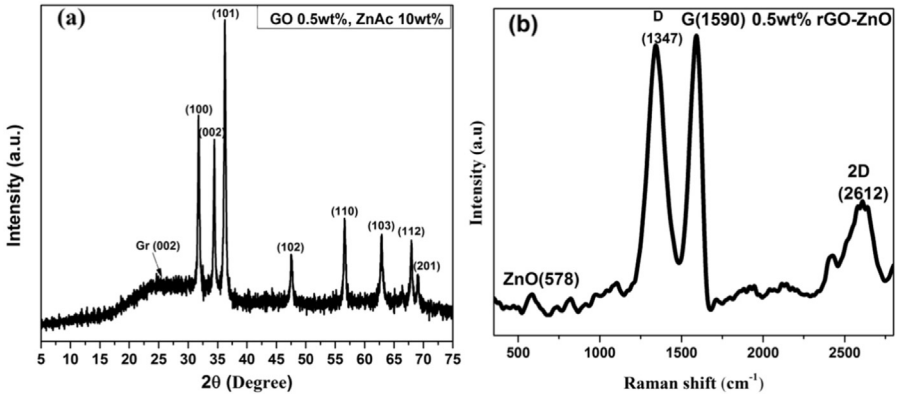

Fig. 2. (a) XRD pattern and (b) Raman spectrum of rGO–ZnO composite.

wide electrochemical potential window, non-toxicity, high chemical stability, and high-electron transfer rate [15,16]. In particular, it has been used for phenol sensing by dielectric manipulation [17]. Similarly, graphene and related materials (such as graphene oxides) exhibit excellent electrochemical sensing ability [18]. In this case, the rGO-ZnO composite was synthesized and subsequently used for phenol sensing. The energy difference between ZnO (large band gap) and rGO (small band gap) was used to form nano-Schottky barriers at the rGO-ZnO junction which can be modulated by the oxidation or reduction of electrochemical species. The oxidation of phenol results in the release of electrons at the electrode surface whose energy is greater than the Fermi level of rGO. Since, the work function of ZnO is greater than that of rGO, electrons jump from the conduction band of ZnO to rGO. Due to the higher mobility in rGO, these electrons are transferred to the GCE. With the successive addition of phenol, the concentration of electrons increases which makes the nano-Schottky barrier forward biased, thereby, increasing the current. The exhibited higher sensitivity, the lower limit of detection and reproducibility of the rGO-ZnO modified electrode towards phenol oxidation are due to the synergistic effects of rGO and ZnO, in terms of excellent charge separation due to the formation of nano Schottky barrier. The rGO-ZnO composite modified GCE sensor provides a simple, non-enzymatic, and low cost detection of phenol in industrial, bio-medical and environmental processes. The property of excellent charge separation due to the formation of nano Schottky barrier at rGO-ZnO interface paves the way for the easy fabrication and testing of rGO-ZnO based environmental sensors for the detection of other phenolic compounds such as 2-Chlorophenol, 2-Nitrophenol, 2,4-Dichlorophenol and other toxic organic pollutants. To the best of our knowledge, no other studies have been reported on rGO-ZnO composite based non-enzymatic phenol sensor.

2. Experimental

2.1. Materials

Concentrated sulfuric acid (H_2SO_4, 98%), phenol (C_6H_5OH), Graphite powder, ethanol (C_2H_5OH), *N*, *N*-dimethylformamide (DMF) ($(CH_3)_2NC(O)H$),

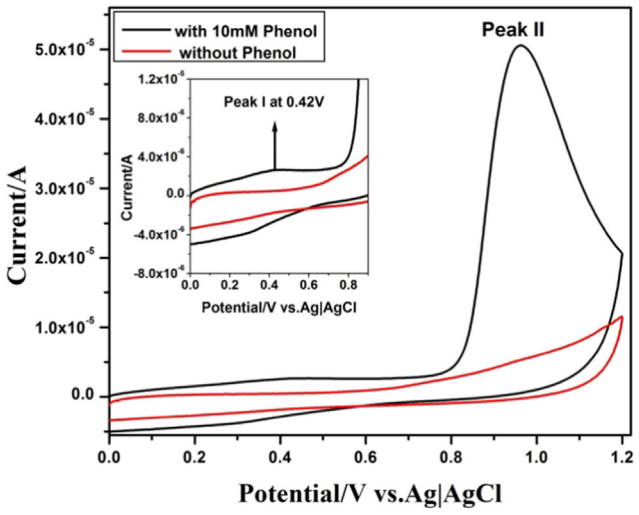

Fig. 3. CV plots of rGO-ZnO modified GCE in the absence of phenol and presence of 10 mM phenol. The inset shows magnified image of peak I.

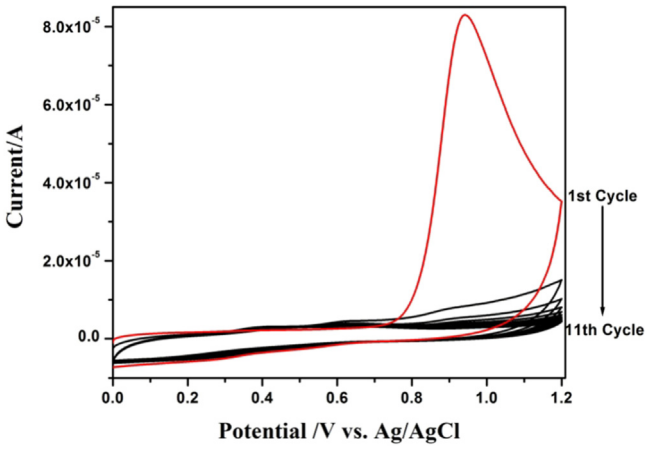

Fig. 4. CV plots of rGO-ZnO modified GCE during cycling in the presence of 10 mM phenol.

and zinc acetate dihydrate (ZnAc) ($Zn(CH_3COO)_2 \cdot 2H_2O$) were procured from Sigma-Aldrich and used directly in the experiments.

2.2. Synthesis of GO and rGO-ZnO nano composite

GO was synthesized by modified Hummers method as described in our previous work [19]. The rGO–ZnO composite was synthesized using a modified in situ wet chemistry method which was previously reported [20]. In brief, 0.5 wt.% of GO was uniformly dispersed in DMF whilst 10 wt.% of ZnAc was dissolved in DMF by ultra-sonication for 2 h and 5 min, respectively. Then GO-DMF solution was added to ZnAc-DMF solution under continuous ultra-sonication. The resultant solution was then heated for 5 h in an oven at a constant temperature of 95 °C and then cooled to room temperature. Subsequently, the resultant solution was centrifuged (at 10,000 rpm) to obtain a solid residue (after discarding the supernatant), which was washed with ethanol and DI water and then dried at 60 °C for 12 h. In the final step, the dried solid was calcined at 400 °C for 1 h to obtain the final product.

2.3. Characterization of materials

Morphology of the as-synthesized materials was characterized by field emission scanning electron microscope (FESEM) operated at an accelerating voltage of 5 kV. Crystal structure of the samples was determined by X-ray diffraction (XRD) whilst the phase information of the samples was studied by Raman scattering. XRD experiments were performed using Cu Kα (wavelength 1.54 Å) line on X'pert PRO X-ray diffractometer. XRD patterns were recorded in the 2θ range 5–75°, θ being Bragg's diffraction angle. Raman spectra were collected in the spectral range 500–3000 cm^{-1} using 532 nm excitation source on Senterra, Bruker spectrometer.

2.4. Sensor fabrication and testing

The calcined sample (i.e., rGO-ZnO composite) was dissolved in DMF, and the resultant solution was continuously stirred at 750 rpm for 2 h in order to obtain uniformly dispersed stock solution. 5 μL of the stock solution was drop-casted onto a clean GCE surface. The drop casted GCE was then dried for 10 min in an oven at 60 °C to obtain rGO–ZnO modified GCE, which was used as a phenol sensor. Three such sensors were fabricated using stock solutions prepared with the three different composites. Cyclic Voltammetry (CV) and differential pulse voltammetry (DPV) measurements were performed on a CHI electrochemical workstation (CHI 660E) at room temperature. Three electrode cell configuration in which rGO-ZnO composite modified GCE (3 mm in diameter) as the working electrode, Ag|AgCl electrode as the reference electrode and Pt wire as the counter electrode was used whilst 0.1 M H_2SO_4 solution was used as the electrolyte. The scan rate was 50 mV/s.

3. Results and discussions

The morphology of rGO-ZnO composite at different magnifications is shown in Fig. 1. Fig. 1(a) shows features (typical to that of ZnO particles [21,22]) whose sizes are in the range 250–300 nm. Each of these features is constituted by smaller features in the range 10–20 nm as shown in Fig. 1(b). However, from Fig. 1, any typical features corresponding to rGO could not be identified, which is plausibly due to optimized low amount of GO used during the synthesis. Nonetheless, XRD (Fig. 2) and Raman scattering analysis confirmed the presence of ZnO and rGO in the composite.

XRD pattern and Raman spectrum of the rGO-ZnO composite are shown in Fig. 2(a) and Fig. 2(b), respectively. Very low-intensity XRD peak at $2\theta = 26.5°$ indicates the presence of rGO in the composite [21, 22]. This implies that at the calcination temperature of 400 °C, GO in the reaction mixture is transformed into rGO. Other diffraction peaks in Fig. 2(a) are indexed to crystallographic planes of hexagonal Wurtzite [22,23]. The typical D, G and 2D Raman bands at 1347, 1590 and 2606 cm^{-1}, respectively corresponding to the presence of rGO [21,22] in the composite could be easily identified in Fig. 2(b). Moreover, the intensity ratio I_G/I_{2D} is greater than 1 indicating the few-layered nature of rGO [24]. Additionally, a Raman band at ~578 cm^{-1} in Fig. 2(b) is attributed to the presence of ZnO in the composite [21,25].

The electro-catalytic oxidation of phenol using rGO-ZnO composite modified GCE was determined using CV. As shown in Fig. 3, in the

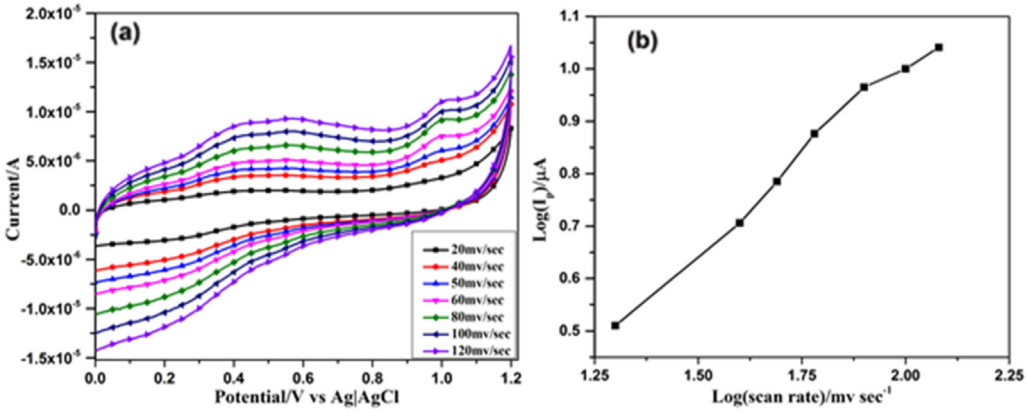

Fig. 5. (a) CV plots of rGO-ZnO modified GCE in the presence of 0.1 mM phenol at various scan rates in the range 20–120 mV/s and (b) the linear relationship between log I_p versus log (scan rate).

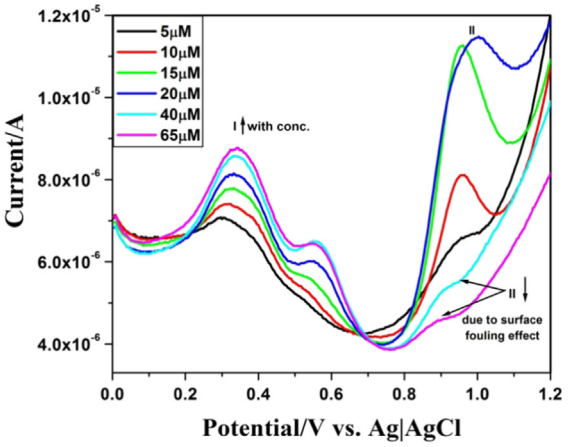

Fig. 6. DPV curves at different concentrations of phenol.

absence of phenol, no well-defined oxidation peaks were identified. In the presence of 10 mM of phenol, a pair of well-defined oxidation peaks was observed at 0.42 (named peak I) and 0.96 V (named peak II), which could be ascribed to the catalytic oxidation of phenol. The identification of oxidation of phenol at a low potential (i.e., at 0.42 V), suggests that the rGO-ZnO modified GCE can be an effective sensor for the detection of phenol. The absence of any reduction peak in CV plots implies that the electrochemical reaction is irreversible. To check any surface fouling effect, rGO-ZnO modified GCE was scanned for several cycles. From Fig. 4, it is clear that the oxidation peak current (at 0.96 V) measured at first cycle is greater than the peak current measured at 11th cycle. The peak current gradually decreased in subsequent cycles. Such drop in the oxidation current is attributed to the electrode's surface fouling. The electro-oxidation of phenol results in the generation of polymerization products and benzenediol isomers, which get deposited on the surface of the electrode, [12,26] and as a consequence deactivate the electrode and prevent any further oxidation of phenol on the electrode's surface.

To select the optimum rGO-ZnO composition for phenol sensing, an optimization study was performed by using three different wt% of GO precursor to synthesize 0.1 wt%, 0.5 wt% and 1 wt% rGO–ZnO composites followed by performing phenol detection. The maximum value of current (peak I) was found in 0.5 wt% rGO-ZnO whilst the value of current obtained in 0.1 wt% rGO-ZnO was the lowest. It could be ascribed to the rapid charge separation at the interface which results in an effective oxidation of phenol at the catalytically active sites of 0.5 wt% rGO-ZnO modified GCE. Hence, to achieve better sensitivity, a 0.5 wt% rGO-ZnO composite was chosen for phenol sensing. Figure that shows the value of current (peak I) measured as a function of different wt% of rGO in rGO–ZnO composite and the detailed optimization study can be found in the Supplementary information (SI) (Fig. S1).

Fig. 5(a) shows the CV plots of rGO-ZnO modified GCE at different scan rates. It is clear from Fig. 5(a) that the two oxidation peak currents increased with the increasing scan rate. To understand the nature of phenol oxidation, i.e., to know if the oxidation is controlled by diffusion or adsorption, the logarithm of peak current (I_p) (here, peak II) has been plotted against the logarithm of scan rate as shown in Fig. 5(b). From the fit data (Fig. 5(b), the following linear relationship between the oxidation peak current and the scan rate is obtained:

$$\text{Log } I_p\ (\mu A) = 0.71 \log(\text{scan rate})\ (\text{mV/s}) - 0.406 \left(\text{correlation co} - \text{efficient}, R^2 = 0.987\right)$$

The value 0.71 of the slope of the linear fit is greater than 0.5 and close to 1, which clearly indicates that the oxidation of phenol on rGO-ZnO modified GCE is controlled by surface absorption process [6]. Since the oxidation of phenol is an adsorption controlled reaction, the by-products of this reaction were easily deposited on the surface, thereby causing surface fouling of the electrode. This observation corroborates well with the decrease in the values of the peak currents with cycling as shown in Fig. 4.

DPV was used for the non-enzymatic detection of different concentrations of phenol using rGO-ZnO modified GCE. Fig. 6 shows the DPV curves for phenol detection. Two anodic peak currents, peak I at 0.35 V and peak II at 0.94 V were clearly observed in Fig. 6. The presence of peak II at 0.94 V indicates the oxidation of phenol to phenoxy radicals by the release of one free electron and one proton at the catalytically active site of the rGO-ZnO modified GCE. Another oxidation peak (peak I) at 0.35 V can be regarded as surface confined hydroquinone's redox species on the surface of the electrode. As shown in Fig. 6, the current of peak II increased only at lower concentrations of phenol (up to 20 μM) and started decreasing at higher phenol concentrations because of surface fouling effect. Phenoxy radicals are further oxidized to Hydroquinone which would be adsorbed on the electrode surface. Therefore no further oxidation of phenol is possible [13,14,27]. Herein, the reasons for choosing peak I for the electrochemical detection of phenol were a) peak I increased linearly with all concentrations of phenol, b) peaks I and II were not interfering with each other and c) peak I was not affected by surface fouling.

To compare the electrochemical sensing performances of the electrodes, GCE was modified with pristine ZnO and 0.5 wt% rGO-ZnO respectively. Fig. 7(a) exhibits DPV response of ZnO/GCE and 0.5 wt% rGO–ZnO/GCE electrodes in 0.1 M H_2SO_4 solution containing 10 μM phenol. The current (peak I) of the composite based sensor at 0.35 V is about 1.35 folds greater than that of pure ZnO based sensor which can

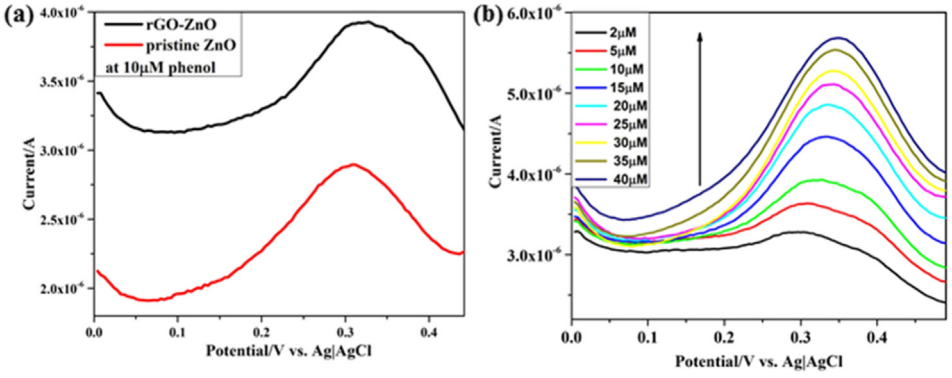

Fig. 7. (a) Comparative DPV response of ZnO/GCE and 0.5 wt% rGO–ZnO/GCE electrodes in 0.1 M H_2SO_4 solution containing 10 μM phenol; (b) DPV responses of 0.5 wt% rGO–ZnO/GCE in 0.1 M H_2SO_4 solution containing different concentrations of phenol; scan rate: 50 mv/s.

be ascribed to the synergistic effects of rGO and ZnO, in terms of excellent charge separation due to the formation of nano Schottky barrier. DPV curves in Fig. 7(b) shows the response of the oxidation peak (peak I) current towards phenol. The oxidation peak current increased with increase in phenol concentration. Fig. 8 presents the calibration plot of DPV curves at different phenol concentrations. Two linear regions were found to occur, i.e., from 2 μM to 15 μM and 15 μM to 40 μM. In the region of 2 μM to 15 μM, the linear regression equation is:

Peak current density J_p (μA/cm^2) = 1.79C (μM) + 52.3 (correlation co-efficient, $R^2 = 0.979$) while in the range of 15 μM to 40 μM, peak current density J_p (μA/cm^2) = 0.389C (μM) + 72 ($R^2 = 0.987$). The limit of detection (LOD) was calculated using the following formula, LOD = 3 S/m where, S is the standard deviation of the response, estimated by the standard deviation of y-intercept of the regression line and m is the slope of the calibration curve. The estimated limit of detection was 1.94 μM. In this work, the sensitivity achieved was higher in comparison to previous reports as shown in Table 1.

Stability and reproducibility of the sensor were investigated by performing the DPVs on the 0.5 wt% rGO-ZnO modified GCE. The sensor could be regenerated by washing it with PBS buffer of pH 7.2. The as-renewed sensor retained 83.1% of its initial conductivity after 3 days storage at room temperature, as shown in Fig. 9(a). The stability of the proposed sensor, in the electrolyte containing 5 μM of phenol, was also verified by performing successive differential pulse voltammograms and after ten measurements the relative standard deviation (RSD) was found to be very less, 4.47% only as shown in Fig. 9(b). These results suggest the good stability and reproducibility of the as-fabricated electrode.

The influence of other toxic organic pollutants such as ethanol and 2-Chlorophenol that possibly occur in wastewater on the detection of phenol with rGO-ZnO modified electrode was also examined. In the presence of ethanol and 2-Chlorophenol, the peak currents were observed to increase slightly (as shown in Table 2) because their electroactive functional groups can be oxidized near the potential of phenol. The changes in current response upon adding these compounds were negligible which authenticates superior selectivity of the developed sensor.

To check of the applicability of the proposed method, the as-fabricated rGO-ZnO sensor was used to detect phenol contents in the real sample (potable drinking water). 10 μM and 40 μM phenol were added to the water sample. The recovery of phenol was estimated using the calibration curve. The recovery of 98–109.2% (as shown in Table 3) authenticates the reliability of the developed enzyme-free phenol sensor in real samples.

There have been several reports of phenol sensors. Quynh et al. demonstrated nanoporous gold for phenol detection. Nanoporous gold was synthesized using multi-step, complex synthesis process such as co-sputtering of Au and Si on n-doped Si substrates and dealloying this AuSi thin films using electrochemical etching in 3% HF solution [2]. Guix et al. presented MWCNTs for phenol detection wherein, it requires one extra CNTs functionalization step to achieve the well dispersed CNTs in a suitable solvent, prior to the modification of the bare electrode with MWCNTs [3]. Beitollahi et al. demonstrated benzoyl ferrocene (BF)/ionic liquid (IL) modified GO nano-sheets paste electrode for the determination of phenol which involves complex sensor fabrication method. To obtain maximum peak current intensity during sensing, a uniformly wetted paste is required with the optimum ratio of BF, IL and GO [33]. Negash et al. reported the synthesis of PEDOT/SWCNTs using two steps which included the electrodeposition of PEDOT on bare GCE followed by drop casting and drying of SWCNTs dispersion onto PEDOT modified GCE [30]. In the literature, different strategies have been used to overcome surface fouling while detecting phenols. For example, Lu et al. developed poly-pyrrole modified electrodes for phenol detection at a constant potential of +1 V [34] and to overcome the surface fouling effect, o-amino-benzesulfonic acid (containing hydrophilic groups) was *co*-electro-polymerized with pyrrole monomer. More recently, Rana et al. reported a pre-charged graphite pencil electrode (pCGPE) for phenol sensing using sophisticated and complex sensor fabrication techniques which included two steps: (1) charging of GPE surface in 0.1 M NaOH solution using CV in the potential range of 1.3 V–1.9 V for 50 segments and (2) formation of additional electroactive layer on the surface of pCGPE using the open-circuit electropolymerization of phenol [35]. However, to retain the electro-activity of the sensor, the electro-polymerization of phenol on the surface of pCGPE was essential before using the electrode for the sensing of phenol. This work demonstrates phenol sensing at lower potential (0.35 V) and this aspect can be easily integrated into device level for real-time low power sensing applications.

Unlike most of the methods mentioned above, which involve complex synthesis procedures, sensor fabrication or detection technique, this method employs a simple, cost effective approach for phenol detection and more importantly eliminates the surface fouling effect by allowing precise selection of the sensing peak, thereby ensuring repeatability. The use of this phenol sensor is beneficial because renewing the surface of the electrode before every scan is not required to achieve reproducible results during phenol sensing. Also, the as-fabricated sensor offers a significantly higher sensitivity with an excellent repeatability, selectivity and stability when compared to the performance of other reported phenol sensors as shown in Table 1. Kane et al. developed phenol

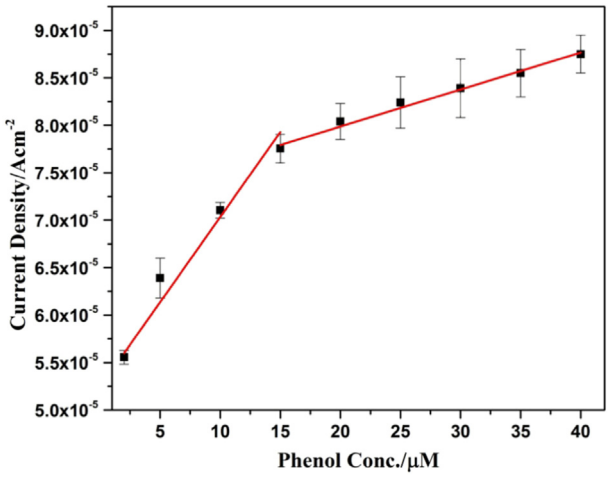

Fig. 8. Calibration curve representing the response of electrodes towards phenol.

Table 1
Comparison in performance of phenol sensors with other reported phenol sensors.

Electrodes	Sensitivity	LOD
Tyrosinase-MWCNT[a]/SPE[b]	1.5 μA/μM cm^2	1.35 μM [3]
Poly(zincon) electrode	0.0245 μA/μM cm^2	9 μM [6]
NPG[c] thin film	350 nA/ μM cm^2	0.1 μM [2]
Tyrosinase-ZnO nanorods/Au	103.08 nA/μM	0.623 μM [28]
Polyacrylamide microgels/GCE	41.36 mA/M cm^2	1.4 μM [29]
MWNT-Nafion-Tyr/GCE	303 μA/mM	0.13 μM [11]
SWCNT[d]/PEDOT/GCE	0.253 μA/μM cm^2	0.094 μM [30]
Boron-doped diamond film	–	1.82 μM/L [4]
H_2 plasma-pre-treated BDND	–	85 μM [31]
Tyrosinase-BiNPs[e]/SPE[b]	14 nA/μM	62 nM [32]
Ionic liquids/GO nanosheets/CPE[f]	0.038 μA/μM	– [33]
pCGPE[g]	–	4.17 nM [35]
rGO-ZnO NPs	1.79 μA/μM cm^2 (2–15 μM)	1.94 μM
	0.389 μA/μM cm^2 (15–40 μM)	This work

[a] MWNT: multiwall carbon nanotubes.
[b] SPE: screen-printed electrode.
[c] Nanoporous gold.
[d] SWCNT: single wall carbon nanotubes.
[e] bismuth nanoparticles.
[f] CPE: carbon paste electrode.
[g] pCGPE: pre-charged disposable graphite pencil electrode.

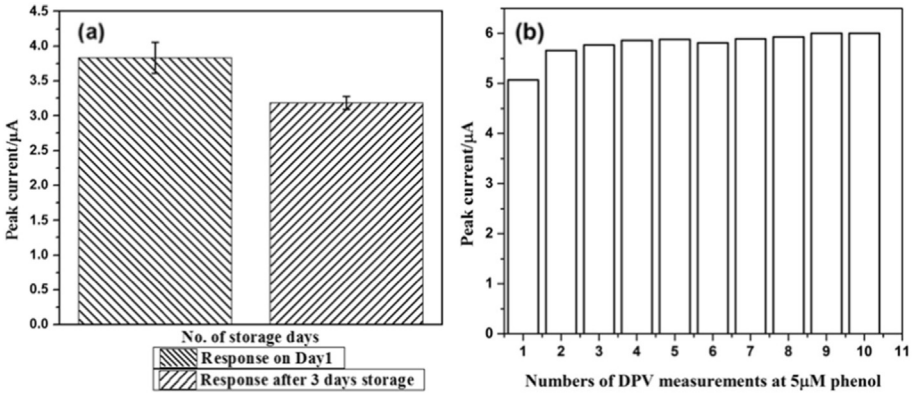

Fig. 9. (a) Peak current of the 0.5 wt% rGO-ZnO modified electrodes measured (1) on day1 and (2) after 3 days storage, showing the stability of the devices; (b) Graph demonstrating stability study of the peak current of ten successive differential pulse voltammograms of the similar rGO-ZnO modified electrode in the electrolyte containing 5 μM of phenol with RSD of 4.47% only.

Table 2
Influence of other toxic organic pollutants on the determination of 10 μM phenol in 0.1 M H_2SO_4 solution.

Interference	Concentration (μM)	Change in the peak current (%)
Ethanol	10	+1.51
2-Chlorophenol	10	+3.95

sensor wherein the response of their sensor was decreased by 50% after 3 days storage [36]. The limit of detection of the developed sensor is 1.94 μM which is sufficient for monitoring phenol in industrial, biomedical and environmental applications.

4. Conclusions

In summary, a novel, relatively simpler method was developed for non-enzymatic phenol detection using rGO-ZnO composite modified GCE which eliminates the surface fouling effect by allowing precise selection of the sensing peak. The proposed sensor has higher sensitivity, stability, reusability, selectivity and lower limit of detection (1.94 μM). The use of this phenol sensor is beneficial because renewing the surface of the electrode before every scan is not required to achieve reproducible results during phenol sensing. The sensor responded linearly to phenol over two ranges: one in the range 2–15 μM ($R^2 = 0.979$) with a ultrahigh sensitivity of 1.79 μA/μM cm^2 and the other in the range 15–40 μM ($R^2 = 0.987$) with a sensitivity of 0.389 μA/μM cm^2. These results can be attributed to excellent charge separation due to the formation of nano Schottky barrier at rGO-ZnO interface, resulting from the difference in work function between them. This novel highly-sensitive rGO–ZnO sensor can be used for a low cost and voltammetric the detection of other phenolic compounds such as 2-Chlorophenol, 2-Nitrophenol, 2,4-Dichlorophenol and other hazardous pollutants.

Supplementary data to this article can be found online at http://dx.doi.org/10.1016/j.jelechem.2016.12.001.

Table 3
Quantification of phenol in potable drinking water using developed sensor via recovery method.

Phenol added (μM)	Phenol recovered (μM)[a]	Relative standard deviation (%)	Recovery (%)
10	10.92	1%	109.2%
40	39.2	1.68%	98%

[a] Average of three measurements.

Acknowledgements

The authors acknowledge the financial assistance from the Department of Science and Technology (DST), Government of India (DST/INSPIRE/04/2014/015132), under INSPIRE Fellowship 2015 and Scientific and Engineering Research Board (SERB) Grant # YSS/2015/000863-SERB.

References

[1] G. Busca, S. Berardinelli, C. Resini, L. Arrighi, Technologies for the removal of phenol from fluid streams: a short review of recent developments, J. Hazard. Mater. 160 (2) (2008) 265–288.
[2] B.T.P. Quynh, J.Y. Byun, S.H. Kim, Non-enzymatic amperometric detection of phenol and catechol using nanoporous gold, Sensors Actuators B Chem. 221 (2015) 191–200.
[3] M. Guix, B. Pérez-López, M. Sahin, M. Roldán, A. Ambrosi, A. Merkoçi, Structural characterization by confocal laser scanning microscopy and electrochemical study of multi-walled carbon nanotube tyrosinase matrix for phenol detection, Analyst 2010 (1918-1925) 135(8).
[4] G.H. Zhao, Y.T. Tang, M.C. Liu, Y.Z. Lei, X.E. Xiao, Direct and simultaneous determination of phenol, hydroquinone and nitrophenol at boron-doped diamond film electrode, Chin. J. Chem. 25 (10) (2007) 1445–1450.
[5] N. Jović-Jovičić, Z. Mojović, M. Darder, P. Aranda, E. Ruiz-Hitzky, P. Banković, ... A. Milutinović-Nikolić, Smectite-chitosan-based electrodes in electrochemical detection of phenol and its derivatives, Appl. Clay Sci. 124 (2016) 62–68.
[6] W. Qin, X. Liu, H. Chen, J. Yang, Amperometric sensors for detection of phenol in oilfield wastewater using electrochemical polymerization of zincon film, Anal. Methods 6 (15) (2014) 5734–5740.
[7] K.R. Rogers, J.Y. Becker, J. Cembrano, S.H. Chough, Viscosity and binder composition effects on tyrosinase-based carbon paste electrode for detection of phenol and catechol, Talanta 54 (6) (2001) 1059–1065.
[8] V. Janda, K. Krijt, Recovery of phenols from water by continuous steam distillation-extraction, J. Chromatogr. A 283 (1984) 309–314.
[9] S.Y. Sheikheldin, T.J. Cardwell, R.W. Cattrall, M.D.L. de Castro, S.D. Kolev, Determination of phenol in water by pervaporation-flow injection analysis, Anal. Chim. Acta 419 (1) (2000) 9–16.
[10] J. Kronholm, P. Revilla-Ruiz, S.P. Porras, K. Hartonen, R. Carabias-Martinez, M.L. Riekkola, Comparison of gas chromatography–mass spectrometry and capillary electrophoresis in analysis of phenolic compounds extracted from solid matrices with pressurized hot water, J. Chromatogr. A 1022 (1) (2004) 9–16.
[11] Y.C. Tsai, C.C. Chiu, Amperometric biosensors based on multiwalled carbon nanotube-Nafion-tyrosinase nanobiocomposites for the determination of phenolic compounds, Sensors Actuators B Chem. 125 (1) (2007) 10–16.
[12] H. Yi, K. Wu, S. Hu, D. Cui, Adsorption stripping voltammetry of phenol at Nafion-modified glassy carbon electrode in the presence of surfactants, Talanta 55 (6) (2001) 1205–1210.
[13] R.H. Carvalho, F. Lemos, M.A.N.D.A. Lemos, J.M.S. Cabral, F.R. Ribeiro, Electrooxidation of phenol on zeolite/graphite composite electrodes: part 1. Electrochemical behaviour over NaY zeolite, J. Mol. Catal. A Chem. 248 (1) (2006) 48–52.
[14] M. Gattrell, D.W. Kirk, A study of electrode passivation during aqueous phenol electrolysis, J. Electrochem. Soc. 140 (4) (1993) 903–911.
[15] A.M. Ali, F.A. Harraz, A.A. Ismail, S.A. Al-Sayari, H. Algarni, A.G. Al-Sehemi, Synthesis of amorphous ZnO–SiO_2 nanocomposite with enhanced chemical sensing properties, Thin Solid Films 605 (2016) 277–282.
[16] S. Ameen, M.S. Akhtar, H.S. Shin, Low temperature grown ZnO nanotubes as smart sensing electrode for the effective detection of ethanolamine chemical, Mater. Lett. 106 (2013) 254–258.

[17] S. Srivastava, A.K. Srivastava, P. Singh, V. Baranwal, R. Kripal, J.H. Lee, A.C. Pandey, Synthesis of zinc oxide (ZnO) nanorods and its phenol sensing by dielectric investigation, J. Alloys Compd. 644 (2015) 597–601.
[18] S. Badhulika, T. Terse-Thakoor, C. Villarreal, A. Mulchandani, Graphene hybrids: synthesis strategies and applications in sensors and sensitized solar cells, Frontiers in Chemistry 3 (2015).
[19] V. Gedela, S.K. Puttapati, C. Nagavolu, V.V.S.S. Srikanth, A unique solar radiation exfoliated reduced graphene oxide/polyaniline nanofibers composite electrode material for supercapacitors, Mater. Lett. 152 (2015) 177–180.
[20] D.I. Son, B.W. Kwon, D.H. Park, W.S. Seo, Y. Yi, B. Angadi, ... W.K. Choi, Emissive ZnO-graphene quantum dots for white-light-emitting diodes, Nat. Nanotechnol. 7 (7) (2012) 465–471.
[21] R.K. Jammula, V.V.S.S. Srikanth, B.K. Hazra, S. Srinath, Strong interfacial polarization in ZnO decorated reduced-graphene oxide synthesized by molecular level mixing, Mater. Des. (2016) (Accepted).
[22] P. Sahatiya, S. Badhulika, One-step in situ synthesis of single aligned graphene-ZnO nanofiber for UV sensing, RSC Adv. 5 (100) (2015) 82481–82487.
[23] M. Shoeb, B.R. Singh, M. Mobin, G. Afreen, W. Khan, A.H. Naqvi, Kinetic study on mutagenic chemical degradation through three pot synthesized graphene@ ZnO nanocomposite, PLoS One 10 (8) (2015), e0135055. .
[24] A. Das, B. Chakraborty, A.K. Sood, Raman spectroscopy of graphene on different substrates and influence of defects, Bull. Mater. Sci. 31 (3) (2008) 579–584.
[25] W.J. Ong, S.Y. Voon, L.L. Tan, B.T. Goh, S.T. Yong, S.P. Chai, Enhanced daylight-induced photocatalytic activity of solvent exfoliated graphene (SEG)/ZnO hybrid nanocomposites toward degradation of reactive black 5, Ind. Eng. Chem. Res. 53 (44) (2014) 17333–17344.
[26] M. Panizza, G. Cerisola, Direct and mediated anodic oxidation of organic pollutants, Chem. Rev. 109 (12) (2009) 6541–6569.
[27] G. Arslan, B. Yazici, M. Erbil, The effect of pH, temperature and concentration on electrooxidation of phenol, J. Hazard. Mater. 124 (1) (2005) 37–43.
[28] B.X. Gu, C.X. Xu, G.P. Zhu, S.Q. Liu, L.Y. Chen, X.S. Li, Tyrosinase immobilization on ZnO nanorods for phenol detection, J. Phys. Chem. B 113 (1) (2009) 377–381.
[29] J.H. Pérez, M.S.P. López, E. López-Cabarcos, B. López-Ruiz, Amperometric tyrosinase biosensor based on polyacrylamide microgels, Biosens. Bioelectron. 22 (3) (2006) 429–439.
[30] N. Negash, H. Alemu, M. Tessema, Determination of phenol and chlorophenols at single-wall carbon nanotubes/poly (3, 4-ethylenedioxythiophene) modified glassy carbon electrode using flow injection amperometry, ISRN Analytical Chemistry (2014).
[31] A.F. Azevedo, F.A. Souza, P. Hammer, M.R. Baldan, N.G. Ferreira, The influence of hydrogen plasma pre-treatment on the structure of BDND electrode surface applied for phenol detection, J. Nanopart. Res. 13 (11) (2011) 6133–6139.
[32] C.C. Mayorga-Martinez, M. Cadevall, M. Guix, J. Ros, A. Merkoçi, Bismuth nanoparticles for phenolic compounds biosensing application, Biosens. Bioelectron. 40 (1) (2013) 57–62.
[33] H. Beitollahi, S. Tajik, P. Biparva, Electrochemical determination of sulfite and phenol using a carbon paste electrode modified with ionic liquids and GO nanosheets: application to determination of sulfite and phenol in real samples, Measurement 56 (2014) 170–177.
[34] W. Lu, G.G. Wallace, M.D. Imisides, Development of conducting polymer modified electrodes for the detection of phenol, Electroanalysis 14 (5) (2002) 325–332.
[35] A. Rana, A.N. Kawde, Open-circuit electrochemical polymerization for the sensitive detection of phenols, Electroanalysis 28 (4) (2016) 898–902.
[36] S. Kane, E. Iwuoha, M. Smyth, Development of a sol–gel based amperometric biosensor for the determination of phenolics, Analyst 1998 (2001-2006) 123(10).